



FULL PAPER

Adaptable Tough Elastomers

An Adaptable Tough Elastomer with Moisture-Triggered Switchable Mechanical and Fluorescent Properties

Xing Zhou, Libing Wang, Zichao Wei, Gengsheng Weng,* and Jie He*

Smart materials with coupled optical and mechanical responsiveness to external stimuli, as inspired by nature, are of interest for the biomimetic design of the next generation of soft machines and wearable electronics. A tough polymer that shows adaptable and switchable mechanical and fluorescent properties is designed using a fluorescent lanthanide, europium (Eu). The dynamic Eu-iminodiacetate (IDA) coordination is incorporated to build up the physical cross-linking network in the polymer film consisting of two interpenetrated networks. Reversible disruption and reformation of Eu-IDA complexation endow high stiffness, toughness, and stretchability to the polymer elastomer through energy dissipation of dynamic coordination. Water that binds to Eu³⁺ ions shows an interesting impact simultaneously on the mechanical strength and fluorescent emission of the Eu-containing polymer elastomer. The mechanical states of the polymer, along with the visually optical response through the emission color change of the polymer film, are reversibly switchable with moisture as a stimulus. The coupled response in the mechanical strength and emissive color in one single material is potentially applicable for smart materials requiring an optical readout of their mechanical properties.

1. Introduction

In nature, biological materials present interesting optical and mechanical responsiveness upon the change in the stress level or local environment, e.g., the color/mechanical strength change of octopus skins when being aggressive^[1] and the open of pinecones when drying.^[2] Numerous biomimetic smart

materials have been developed with similar adaptable properties in response to external stimuli. In such a system, synthetic materials consist of dynamic interactions, e.g., hydrogen bonding,^[3] coordination,^[4] hydrophobic interaction,^[5] and dynamic covalent bond,^[6] that allow the reshape of the structure and the change of composition of materials under external stimuli.^[6,7] The disruption and reformation of dynamic interactions enable the switchability in different mechanical states, usually weak and strong, respectively. One example is the use of the catechol-Fe³⁺ coordination in a pH responsive hydrogel.^[4a] The disruption of catechol-Fe³⁺ coordination under acid condition weakens the physical cross-linking network, thus softening the hydrogel. Integrating optical and mechanical response in the same material, however, is technically challenging yet would

[8]

be highly desirable. In particular, the coupling of optical and mechanical response

in one material potentially adds in visualizable readout on its mechanical strength by color change under external stimuli.

Lanthanides like Eu and Tb show intense fluorescence in visible range, particularly when coordinated with sensitizing ligands as “antenna” in their coordination environment.^[9] Lanthanide metals usually have large coordination numbers (9–12) with preferentially binding to more electronegative elements, e.g., O.^[10] For example, Eu complexes can pick up trace amount of water from organic solvents, which has been widely studied for water detection on the basis of the fluorescence quenching.^[11] By incorporating red-emissive Eu³⁺ ions in the polymer matrix, others and our group have shown that the responsiveness of polymers can modulate the fluorescent emission of Eu³⁺ ions.^[4b,9a,12] In the current contribution, the dynamic coordination of Eu-iminodiacetate (IDA) as a key component is used to build up the physical cross-linking network in the polymer film consisting of interpenetrating polymer network (IPN) (**Figure 1a**). The disruption/reformation of Eu-IDA complexes not only switches the mechanical states of the polymers, but also brings the visually optical response through the emission color change of Eu³⁺ ions; that is, the coupled response in mechanics and optics are integrated in one polymer. We use IDA-containing poly(di(ethylene glycol) methyl ether methacrylate) (PMEO₂MA) to coordinate Eu³⁺ ions and

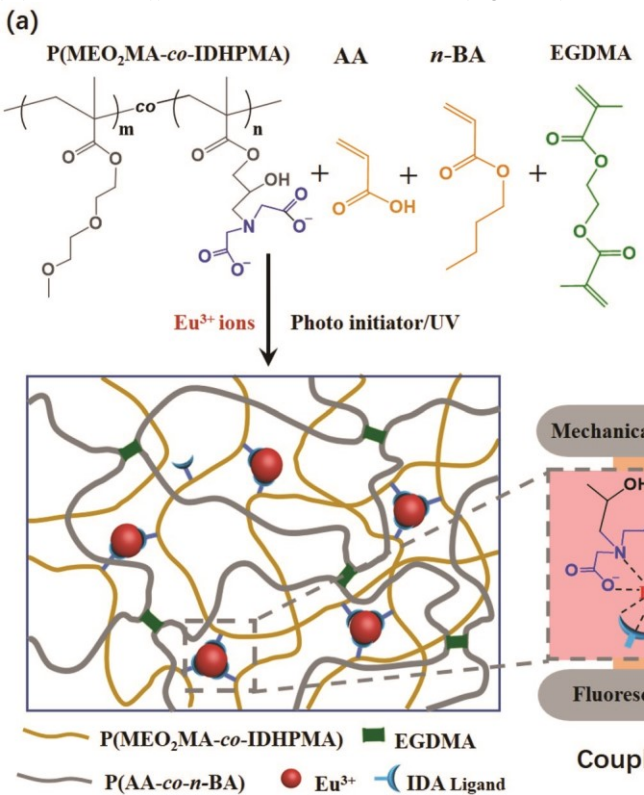
X. Zhou, L. Wang, Prof. G. Weng
School of Materials Science and Chemical Engineering
Ningbo Key Laboratory of Specialty Polymers
Ningbo University
Ningbo 315211, China
E-mail: wenggengsheng@nbu.edu.cn

Z. Wei, Prof. G. Weng, Prof. J. He
Department of Chemistry
University of Connecticut
Storrs, CT 06268, USA
E-mail: jie.he@uconn.edu

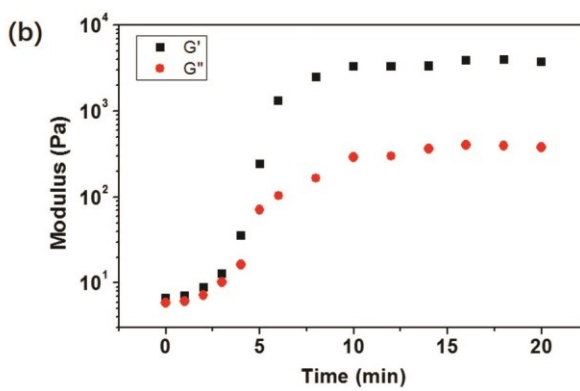
Prof. J. He
Polymer Program
Institute of Materials Science
University of Connecticut
Storrs, CT 06268, USA

The ORCID identification number(s) for the author(s) of this article can be found under <https://doi.org/10.1002/adfm.201903543>.

chemically cross-linked poly(acrylic acid-*co*-*n*-butyl acrylate) (P(AA-*co*-*n*-BA)) as the other covalent network (Figure 1a).



2. Results and Discussion



Coupling of optical and mechanical response

Figure 1. Preparation of the tough elastomer containing two networks. a) Illustration of the preparation method of the IPN elastomer using photopolymerization. P(MEO₂MA-*co*-IDHPMA) coordinates with Eu³⁺ ions to form physical cross-linking network. Monomers of AA and *n*-BA are polymerized in the presence of EGDMA as a chemical cross-linker to form the covalently cross-linked network. The scheme of IPN show the response of Eu-IDA coordination to moisture, pH and Fe³⁺ ions that in turn controls the optical and mechanical properties of the polymer film. b) Storage modulus (G') and loss modulus (G'') plotted against reaction time during the photopolymerization. The organogel was subjected to a small oscillation strain (1%) at an oscillation frequency of 1 rad s⁻¹. c) Optical images to show the transparency of the dried elastomer film with a sample thickness of 0.4 mm (left) and its luminescence under UV light (365 nm). All samples shown in the figure have an IDA-to-Eu ratio of 7/1 (mol/mol).

The coexistence of sacrificial metal coordination bonds along with chemical cross-links results in a tough elastomer. With a low content of Eu³⁺ ions (the mole ratio of IDA-to-Eu 7/1), the elastomer becomes tough. Meanwhile, the Young's modulus (*E*) can reach 24.3 MPa, much stiffer than traditional rubbers with an *E* of around 1 MPa.^[13] The dynamic nature of the Eu-IDA coordination also enables to reversibly tune the coordination by the change of pH, ions and moisture (Figure 1a). We demonstrate that the dissociation of Eu³⁺ ions even upon hydration by moisture can result in the switch off toughness and changing fluorescent color; subsequently, the removal of coordinated water can completely recover its original mechanical strength and fluorescent emission. Our results, as a proof-of-concept, illustrate the bioinspired design of smart polymer elastomeric materials with coupled optical and mechanical responsiveness that will be of interest for biosensors,^[14] wearable optoelectronics,^[15] and anticounterfeiting materials.^[16]

The copolymer of poly(di(ethylene glycol) methyl ether methacrylate-*co*-glycidyl methacrylate) (denoted as P(MEO₂MA-*co*GMA) ($M_n = 127.8 \text{ kg mol}^{-1}$, $D = 3.62$ and the mole ratio of MEO₂MA-to-GMA is 5/1) was prepared through free radical polymerization. A postpolymerization modification was carried out via the ring opening reaction of epoxides with excess sodium iminodiacetate in mixed solvent of methanol/*N,N*'dimethylformamide (10/1, v/v) at 65 °C to yield poly(di(ethylene glycol) methyl ether methacrylate-*co*-3-iminodiacetate-2-hydroxypropylmethacrylate) (denoted as P(MEO₂MA-*co*-IDHPMA)).^[17] The synthetic details and the characterization results of the two polymers are given in the Supporting Information (Figure S1). When adding Eu(NO₃)₃ to the P(MEO₂MA-*co*-IDHPMA) aqueous solution (10 wt%) with an IDA-to-Eu ratio of 7/1 (mol), a clear sol-gel transition was seen (Figure S2a, Supporting Information), suggesting that Eu³⁺ ions can effectively induce the intermolecular cross-linking via the coordination with IDA as reported previously.^[12a]

To prepare the elastomer containing dual networks, acrylic acid (AA), *n*-butyl acrylate(*n*-BA), ethylene glycol dimethacrylate (EGDMA, cross-linker), and 2-hydroxy-2-methyl-1-

phenylpropan-1-one (photoinitiator) were added into the P(MEO₂MA-*co*-IDHPMA) solution (10 wt% in methanol/dioxane, 10/1, v/v). The weight ratio of (P(MEO₂MA-*co*IDHPMA): AA: *n*-BA:EGDMA is 10: 27: 6: 0.75 in the final solution. To this solution, a predetermined amount of Eu(NO₃)₃ (the mole ratio of IDA-to-Eu 7/1 was used as an example and the same ratio was used throughout unless otherwise stated) was further added where the gelation occurred immediately due to the formation of Eu-IDA coordination. After incubation for 5 h at room temperature, the organogel was further exposed to UV light (1 mW cm⁻², 365 nm) to polymerize AA, *n*-BA and EGDMA. The copolymerization of AA and *n*-BA in the presence of EGDMA as a chemical cross-linker resulted in the formation of the second network in the organogel.

To evidence the formation of the second network, the photopolymerization was monitored using a rheometer. The organogels subject to UV irradiation were studied using constant oscillating measurements (a strain of 1% at a frequency of 1 rad s⁻¹) at 25 °C to obtain the storage modulus (G') and the loss modulus (G''). G' and G'' plotted against the irradiation time are shown in Figure 1b (see Figure S4 for details in the Supporting Information). Before photopolymerization, the organogel is weak with a G' of 6.6 Pa. After photopolymerization for 3 min, both G' and G'' increased sharply. It took around 10 min to reach a modulus plateau where G' is significantly higher than G'' . All photopolymerization was conducted for 20 min to ensure the high conversion of monomers and cross-linkers. For the organogel with of an IDA-to-Eu ratio of 7/1, G' reaches to 3.7 kPa, nearly three orders of magnitude higher than that before photopolymerization. Those results indicate the formation of another chemically cross-linked network, or the IPN in organogels. The organogels have a thickness of around 1 mm and a diameter of 60 mm.

The resulting organogels can further be dried to remove methanol and dioxane to form elastic films. The films are highly transparent (Figure 1c) and display a large shrinkage of volume, compared to that of organogels. The small angle X-ray scattering (SAXS) profile for the Eu-containing elastomer film does not show any scattering peak (Figure S5, Supporting Information), implying that there is no electron density fluctuation at nanoscale. It indicates that Eu-IDA complexes do not phase separate in the polymer matrix. After drying, the films have a thickness of 0.4 mm and the diameter only had a slight decrease (<2 mm). The obtained IPN elastomers (IDA-to-Eu ratio of 7/1) have a G' of 32 MPa (measured by a dynamic mechanical analyzer (DMA), see the Supporting Information for more details), which is four orders of magnitude higher than the organogels. The overall quantum yield of the Eu-centered luminescence in this elastomer film is $4.7 \pm 0.1\%$.^[18] The emission decay was best fitted as a biexponential decay (Figure S6, Supporting Information)^[12d] to obtain fluorescence lifetimes, $\tau_1 = 0.18$ ms (37%) and $\tau_2 = 0.51$ ms (63%). The disk-like elastomer films can be cut into desired geometries for further measurements.

Compared to the chemical cross-linking network generated by photopolymerization, the coordination of Eu-IDA as the physical cross-linking network is dynamic. Upon mechanical deformation, the reversible dissociation and reformation of the Eu-IDA complexation can dissipate energy. The impact of the Eu-IDA complexation on the mechanical properties of the elastomer was

first investigated using uniaxial tensile tests. In the absence of Eu³⁺ ions, the mechanical properties of the film of P(MEO₂MA-*co*-IDHPMA) mixed with the P(AA-*co*-*n*-BA) is weak with a tensile strength of 0.5 MPa, an E of 2.2 MPa and an elongation at rupture of 320%. At an IDA-to-Eu ratio of 7/1, the stress-strain curve shows a pronounced increase in stiffness where the E (calculated from low-strain region (<3%)) of Eu-containing elastomers reaches 24.3 MPa (Figure 2a), which indicates the high binding strength of the metal-ligand interaction. Subsequently, it shows a large deformation after the initial yielding, which is similar to those elastomers with high toughness.^[12,19] Comparing to the elastic film without Eu³⁺ ions, the tensile strength of Eu-containing IPN elastomer increased 440% to 2.7 MPa with a slightly larger elongation at rupture of 390%.

We further investigated the stress relaxation behavior. The films with and without Eu³⁺ ions were both stretched to a strain of 100% and immediately hold for 20 min to measure the change of stress (normalized by σ_{\max} , the stress at the beginning of relaxation) versus time. As shown in Figure 2b, the stress of both samples decayed as time elapsed, indicating the release of stress. The Eu-containing film released 85% of stress in the first 5 min, while the sample without Eu³⁺ ions released 60% of stress. Due to the dynamic nature of the coordination of Eu-IDA, the physical cross-linking network can endure large deformation and undergo fast recovery by reforming the complexation of Eu-IDA. As it is stretched and hold for relaxation, the coordinated Eu-IDA complexes break down and then quickly reform at newly accessible sites resulting in a fast release of stress, i.e., stress relaxation and dissipation of energy.^[13c,19b,c,20]

Cyclic loading-unloading measurements were used to examine the strain-history dependence, as well as the toughness of the films. When the elastomer film was stretched to a strain of 200% and unloaded immediately (Figure 2c), a residual strain of 70% in the retraction process was observed. The residual strain originates from the breaking of coordination bonds during stretching. During the immediate reloading process, a residual strain of only 4% was observed (96% recovery of strain, compared to the initial cycle). It implies that broken coordination bonds reformed at newly accessible sites and only a small amount of stress-free network chains remained.^[13c,19b] In the consecutive loading-unloading cycles, residual strain in the retraction process was always $\approx 70\%$ regardless of the rest time, indicating that the covalent network and the residual unchanged coordination preserve shape memory. Similarly, the stress was 86% recovered for immediate reloading and 94% recovered in a short rest time of 5 min. It is noteworthy that the stress at the strain of 200% was restored with a resting interval of 30 min, although the area of the hysteresis loop was smaller than the original one. Upon cyclic loading of the double network, the energy dissipation is reflected by hysteresis loops as strains beyond the linear regime, also known as the toughness. We calculated the energy dissipation (the area of the hysteresis loop as given in Figure 2d) from the cyclic loading curves in Figure 2c. The energy dissipation of the first cycle is 1.51 J cm⁻³. A 0.91 J cm⁻³ of energy dissipation was seen for immediate reloading (60% recovery of toughness). As the rest time increased, more toughness was recovered. After 30 min, 82% toughness was recovered. The strain-

history dependence of the polymer film without Eu ions was also measured and shown in Figure S7 (Supporting Information), where we did not see gradual recovery of toughness in a rest time of 5, 10, and 30 min. Since P(MEO₂MA-*co*-IDHPMA) was uncrosslinked, a relatively large residual strain of $\approx 25\%$ was seen after the first cyclic loading. These findings suggest a good recovery of toughness due to the dynamic coordination of Eu-IDA.

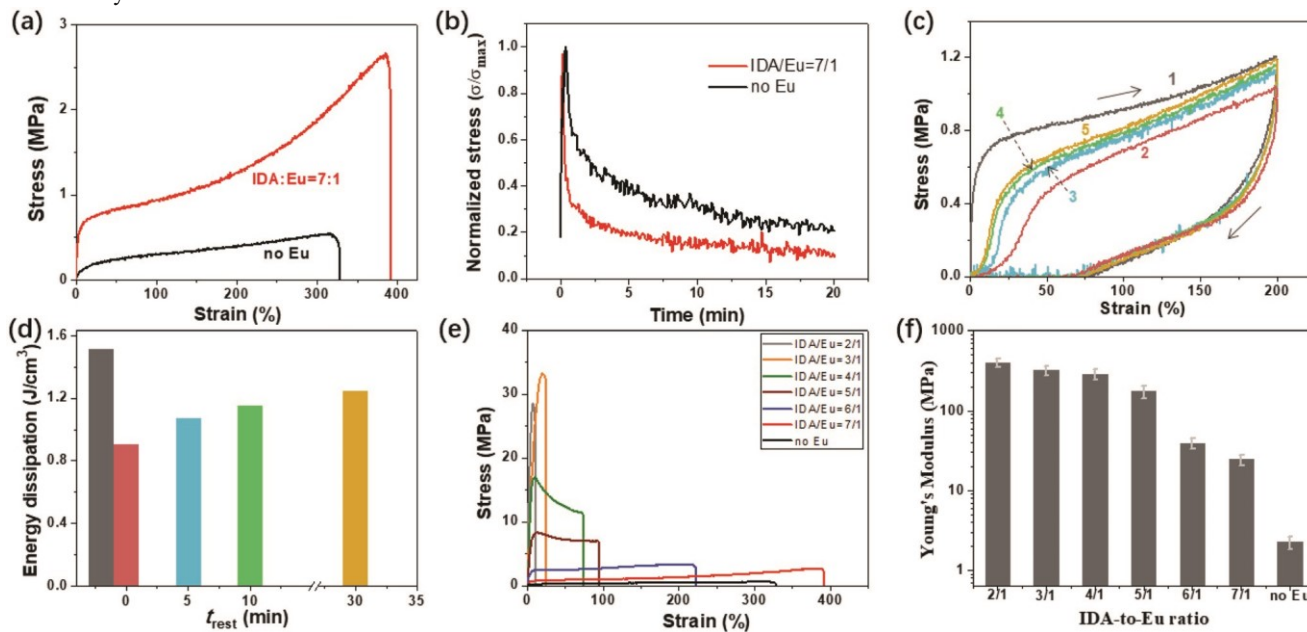


Figure 2. Mechanical properties of the Eu-containing tough elastomers. a) Tensile stress curves of the elastomer without Eu³⁺ ions (black) and Eu-containing elastomer (red). b) Stress relaxation of the elastomers without Eu³⁺ ions (black) and Eu-containing (red). Both samples were stretched to a strain of 100% and σ_{\max} is the stress at the beginning of relaxation. c) Cyclic stress-strain measurement showing the strain-history dependence of the Eu-containing IPN elastomer with various rest intervals (1: original; 2: 0 min; 3: 5 min; 4: 10 min; 5: 30 min). The immediate reloading shows nearly 100% strain recovery. d) Histogram of toughness calculated from (c). e) Tensile stress curves of the elastomers prepared with different IDA-to-Eu ratios showing the influence of the Eu³⁺ content on the mechanical properties. f) Histogram of Young's modulus (E) versus the ratio of IDA-to-Eu. All elastomer films have a thickness of 0.4 mm, width of 10 mm, length 30 mm, and the loading rate of 50 mm min^{-1} is used throughout the measurements.

As the content of Eu³⁺ ions increased, stiffening of the elastomer can be seen (Figure 2e,f). When the IDA-to-Eu ratio was down to 4/1, the significant increase of the E was seen. With a higher concentration of Eu³⁺ ions, a gradual transition from elastic to plastic was noted, since the stress decreased gradually after yielding and the E dramatically increased to 288 MPa at an IDA-to-Eu ratio of 4/1. Further increase of the content of Eu³⁺ ions would result in the formation of the brittle films where only plastic deformation and low elasticity was observed (elongation at break below $< 20\%$). The E increased to 397 MPa for the film with an IDA-to-Eu ratio of 2/1. As the amount of Eu³⁺ ions (decreasing of IDA-to-Eu ratio) increased, the physical crosslinking density increased. Since the chemical cross-linking density did not change, the mechanical properties were mainly controlled by the physical cross-linking of IDA-to-Eu coordination. This then resulted in the enhancement of mechanical properties. Therefore, those results indicate the high binding strength of the IDA-to-Eu interaction.^[19a,b] Meanwhile, the loss or retardation of dynamic properties of Eu-IDA complexation when the IDA-to-Eu ratio was higher than 4/1 also contributed to the dramatical increase of E . From the molecular level, this

presumably is due to the lack of the free IDA ligand to recover the coordination of Eu³⁺ ions upon dissociation.

Since the dynamic coordination of Eu-IDA is responsible for the toughness, the toughness of the elastomers was further measured using the cyclic loading-unloading tests at the IDA-to-Eu ratio ranged from 7/1 to 5/1. The toughness estimated from the energy

dissipation of the first cycle is 1.51, 2.21, and 3.78 J cm^{-3} , for elastomers with an IDA-to-Eu ration of 7/1, 6/1, and 5/1, respectively (Figure S8, Supporting Information). However, the recovery rate, i.e., the percentage of toughness recovery upon reloading of the networks, dropped quickly at a higher content of Eu³⁺ ions. For the film with an IDA-to-Eu ratio of 5/1, the toughness recovered only 45% compared to that in its first cycle after a resting interval of 30 min. This, again, suggests that the film with more Eu³⁺ ions becomes too stiff to allow efficient reformation of the dynamic network of Eu-IDA complexation.

The fluorescence emission of Eu³⁺ ions is extremely sensitive to the coordination environment.^[9a,b,c,11,21] Smaller transitional metal ions (e.g., Fe³⁺, Cu²⁺, and Zn²⁺) can be used to compete for the coordination of Eu-IDA as reported in our previous study.^[12a] Since the IDA can accommodate one small metal ion better than the large Eu³⁺ ion, the addition of those smaller transitional metal ions would disrupt the Eu-IDA coordination. This, consequently, will weaken the physical crosslinking network of the IPN elastomers. On the other hand, the dissociation of Eu-IDA complexation will allow water to hydrate the less coordinated Eu³⁺ ion in its first coordination sphere. The strong O-H vibration as “oscillators” can

shorten the lifetime of Eu^{3+} excited state,^[9b] thus leading to the decrease in the fluorescence emission of Eu^{3+} ions. Additionally, the change in pH that protonates the COOH and the tertiary amine groups will bring similar impacts on the coordination and the emission of Eu^{3+} ions.

To demonstrate the coordination competition on the polymer film, we used $\text{Fe}(\text{NO}_3)_3$ solution as an ink to print an “Eu” pattern on the elastomer having an IDA-to-Eu ratio of 7/1. As shown in **Figure 3a**, a clear “Eu” pattern with a yellowish color contrast can

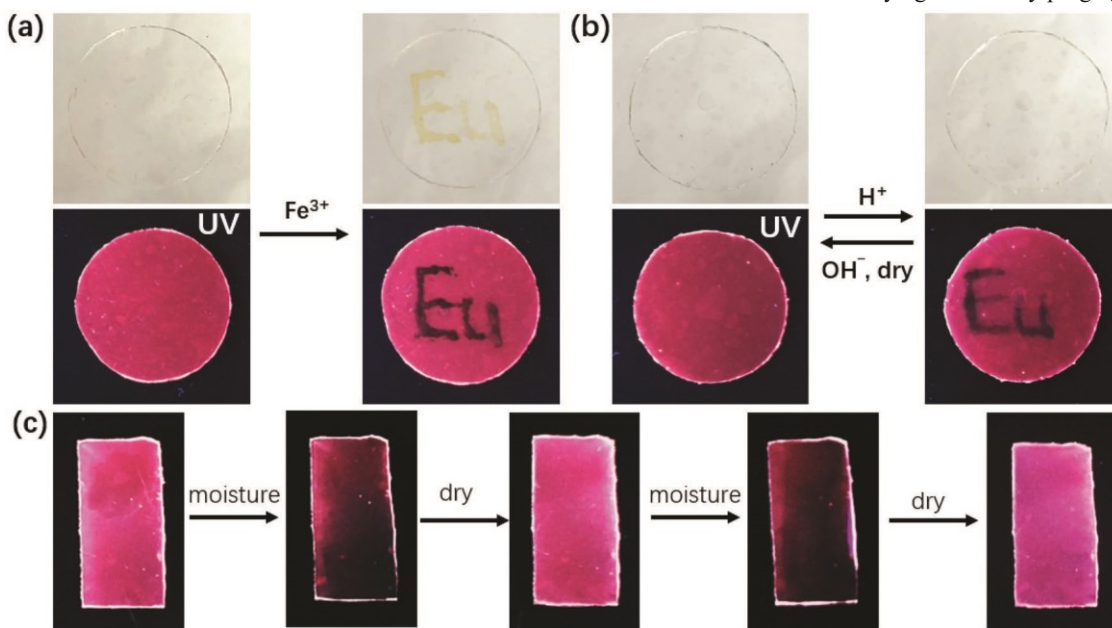


Figure 3. Moisture-controlled optical response of the Eu-containing polymer films upon change in ions, pH and moisture. a,b) Images showing fluorochromic performance on the Eu-containing elastomer by printing “Eu” with $\text{Fe}(\text{NO}_3)_3$ aqueous solution (5 wt%, a) and HCl (1 M, b) as an ink. Fluorescence quenching of Fe^{3+} ions and HCl gave a negative image of “Eu” under UV light (365 nm). The Eu-containing film is “rewritable” when using HCl (1 M) as an ink and NaOH (1 M) as an “eraser.” The printed pattern can be “erased” by NaOH and the fluorescence can be fully recovered after drying. c) Images showing fluorescence ON/OFF response of the elastomer film triggered by moisture (80% of RH) at room temperature.

be seen under sunlight because of the color from Fe^{3+} ions. The change in fluorescence emission of Eu can be visualized by UV light where the printed region appeared to be dark and the unprinted region showed strong red emission (Figure 3a). In comparison to the Fe^{3+} ions as an ink, using of HCl and NaOH solution repeatedly to print on the film makes the film “reprintable” (Figure 3b). With HCl as an ink, the printing is resulted from the fluorescence quenching by protonating the IDA ligands, leading to the dissociation of Eu^{3+} ions to IDA. Erasing of the printed patterns can be achieved by deprotonation of the IDA ligands with NaOH , following by drying to remove residual water. The fluorochromic response of Eu^{3+} ions in turn confirms that the dynamic coordination and dissociation of Eu-IDA complexation in the elastic films can be triggered by external stimuli.

Since the hydration of Eu^{3+} ion is the main cause of its fluorochromic response, we further examined whether water as a guest molecule could vary the coordination environment of Eu^{3+} ions. Previous literatures suggest that water can hydrate Eu compounds to quench the fluorescence; and the fluorescence of hydrated Eu compounds correlates well with the number of water

molecules per Eu^{3+} ions to sense the trace amount of water.^[11c] To study the impact of water on the fluorescence emission, the Eu-containing film was stored under controlled relative humidity (RH). Representative optical images of the elastomer having an IDA-to-Eu ratio of 7/1 under moisture are shown in Figure 3c. A clear moisture-induced fluorescence quenching is seen after exposure to an RH of 80% for 2.5 h. Since the two polymer networks of the IPN elastomers are both hydrophilic, water molecules as moisture can slowly diffuse into the film. The fluorochromic responsiveness to moisture is reversible. After drying the film by purging dry N_2 for

24 h, the bright emission of Eu^{3+} ions could recover completely. In addition, the fluorescence emission is sensitive to the RH. Under less humid conditions, the fluorescence quenching is slower (see Figure S9, Supporting Information).

To verify of fluorochromic responsiveness of the Eu-containing elastomers to moisture, the fluorescence of the elastomers was further studied in the coexistence of fluorescein. Fluorescein has been widely used as a green-emissive dye. When doping fluorescein in the Eu-containing elastomer, the white-luminescent film can be generated by optimizing the ratio of the two fluorophores (see supporting info for details). Compared to the single-red-emissive film, if only Eu emission is turned OFF by moisture, the change in the emission color is visualizable. As given in **Figure 4a**, the polymer film containing Eu ions and fluorescein was yellowish under sunlight and it emitted white light under UV. After stored under an RH of 80% for 2.5 h, the polymer film exhibited a remarkable change of its emissive color from white to green. More qualitatively, the fluorescence spectra of the film were monitored under an RH of 80% every 30 min (Figure 4b). A gradual decrease of the emission peak of Eu^{3+} ions at 617 nm is seen while the broad emission of fluorescein with a peak at 512 nm does not change

under the same condition. Those results indicate that the hydration of Eu ions quenches the red emission while it shows no impact on the green emission of fluorescein.

The change in fluorescence emission of Eu³⁺ ions can be plotted against the exposure time using the emission peak of Eu³⁺ ions at 617 nm. A quasilinear correlation of the emission intensity at 617 nm versus the exposure time can be seen in Figure 4c. The fluorescence emission intensity of Eu³⁺ ions at 617 nm dropped by \approx 50% after 2.5 h. We further recorded

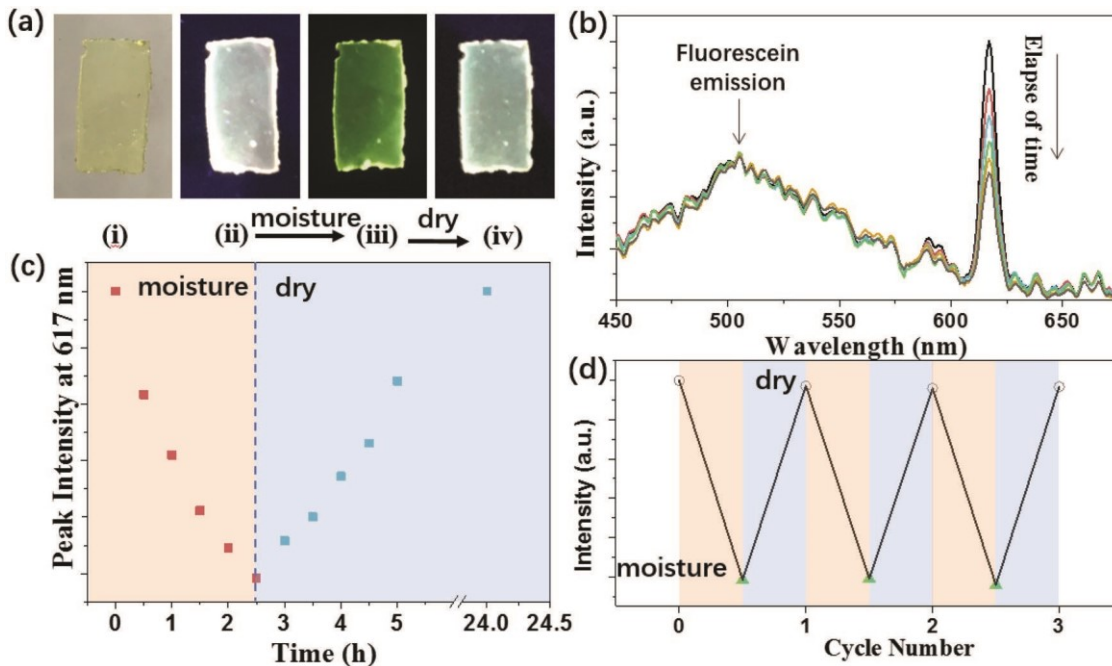
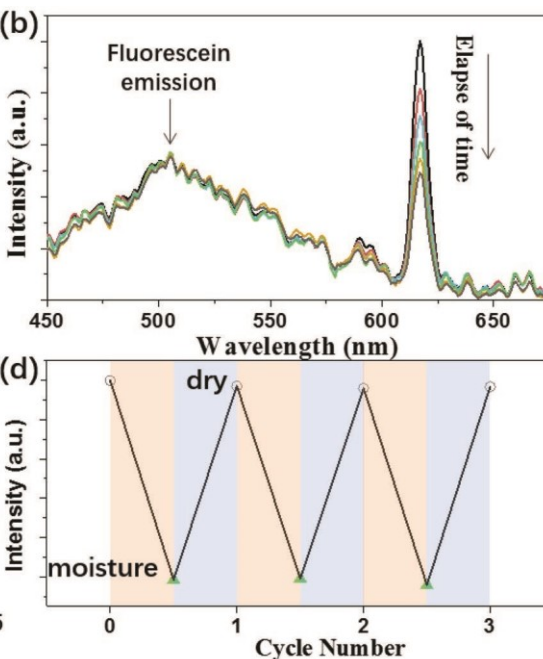


Figure 4. Moisture-controlled fluorochromic response of the polymer film containing Eu³⁺ ions and fluorescein. a) Optical images of the film taken under i) sunlight (left one) and ii–iv) UV light (365 nm, the three images on the right). ii) The polymer film with fluorescein/Eu = 1/46 (mol/mol) is white-emissive. iii) After subject to an RH of 80% for 2.5 h, the emissive color change from white to green can be seen. iv) The white color can be recovered after drying by purging dry N₂. b) Fluorescence emission spectra of the polymer film containing Eu³⁺ ions and fluorescein under an RH of 80% during a time span of 2.5 h. The spectra were taken every 30 min. c) The peak intensity at 617 nm plotted against the exposure time under a moisture-dry cycle. d) Fluorescence ON/OFF of the polymer film by three consecutive moisture-dry cycles. The blue triangles show the fluorescence intensity after hydrated for 2.5 h at an RH of 80%, while the open circles show the fluorescence intensity after drying. The polymer film in this figure has an IDA-to-Eu ratio of 7/1 and a thickness of 0.4 mm. All measurements were carried out at 25 °C.

the reversibility of fluorochromic response of the film under moisture-dry cycles (Figure 4c). The drying of the film was achieved by purging dry N₂ here. It is clear that the fluorescence emission of Eu³⁺ ions at 617 nm can be fully recovered after 22 h. We further measured the fluorescence change in three consecutive moisture-dry cycles (Figure 4d). The ON/OFF switchable emission of Eu³⁺ ions, as well as the emission color change of the film, is fully reversible in response to moisture.

The hydration of Eu³⁺ ions by moisture that results in fluorescence quenching potentially brings the coordination competition with IDA. Since the second network formed by Eu-IDA coordination is mainly responsible for the mechanical robustness of the elastic film, the hydration of Eu³⁺ ions likely weakens the physical cross-linking networks (Figure 5a); thus it further changes mechanical strength and toughness as well. Using Eu-containing elastomer with an IDA-to-Eu ratio of 7/1 as an

example, the mechanical property of the elastomer was measured upon the exposure to moisture (an RH of 80%, Figure 5b). Upon exposure to moisture, the mechanical robustness decreased gradually (Figure S10 for other exposure times). When the film was exposed to such humidity for 1.5 h, the tensile strength decreased significantly from 2.7 to 0.73 MPa, accompanied with a decrease of toughness (fracture energy) from 5.51 to 1.83 J cm⁻². When the sample was exposed for 2.5 h, the tensile strength further decreased to 0.36 MPa, lower than that of the film without Eu³⁺ ions (0.5 MPa).



This is likely because of the slightly plasticizing effect of water to the polymer film.^[22] Meanwhile, the fracture energy decreased to 0.75 J cm⁻². Interestingly, the strain at rupture of the film is minimally impacted by moisture in regardless of the exposure time. This is reasonable since the rupture of the film is mainly dependent on the break of the chemical cross-linking network formed by photopolymerization. In addition, the decrease in E from 24.3 to 0.64 MPa was observed when exposing to moisture for 2.5 h (Figure 5c). Those findings clearly suggest that, i) the film becomes soften by moisture and ii) the mechanical robustness of the film can be switched ON/OFF by moisture, since the water coordination to Eu³⁺ ions is reversible as discussed above.

Now that the mechanical strength, stiffness and toughness of the Eu-containing film are moisture-responsive, moisture as a stimulus can further be used to switch the mechanical states reversibly. As a proof-of-concept, we examined *in situ* the modulus of the film by alternatively purging dry N₂ and moisture-saturated air using DMA.

Both gases are directly purged to the testing chamber while the moduli were measured under dynamic cycles (Figure 5d,e and see the Supporting Information for details). The DMA measurement was carried out under a frequency of 5 Hz and a strain of 1%. Before purging moisture-saturated air, the polymer film shows G' and G'' of 33 and 26 MPa, respectively. The sample is an elastic solid. When purging with moisture-saturated air ($t = 12$ min), both moduli started to decrease. A crossover of G' and G'' occurred after 6 min of moisture purge. G' and G'' reached 10.4 and

= 28 MPa, indicating the recovery of the moduli. The reversible change in G' and G'' of polymer film in response to moisture was examined for 2 cycles. A fully reversible moisturecontrolled switch of mechanical states between “viscous fluid” and “elastic solid” is seen. Additionally, to further clarify the role of water in weakening the mechanical robustness and exclude the influence of plasticizing effect of moisture, the same DMA measurement for the polymer in the absence of Eu^{3+} ions was conducted (Figure S12, Supporting Information). Although we see a similar variation trend of dynamic

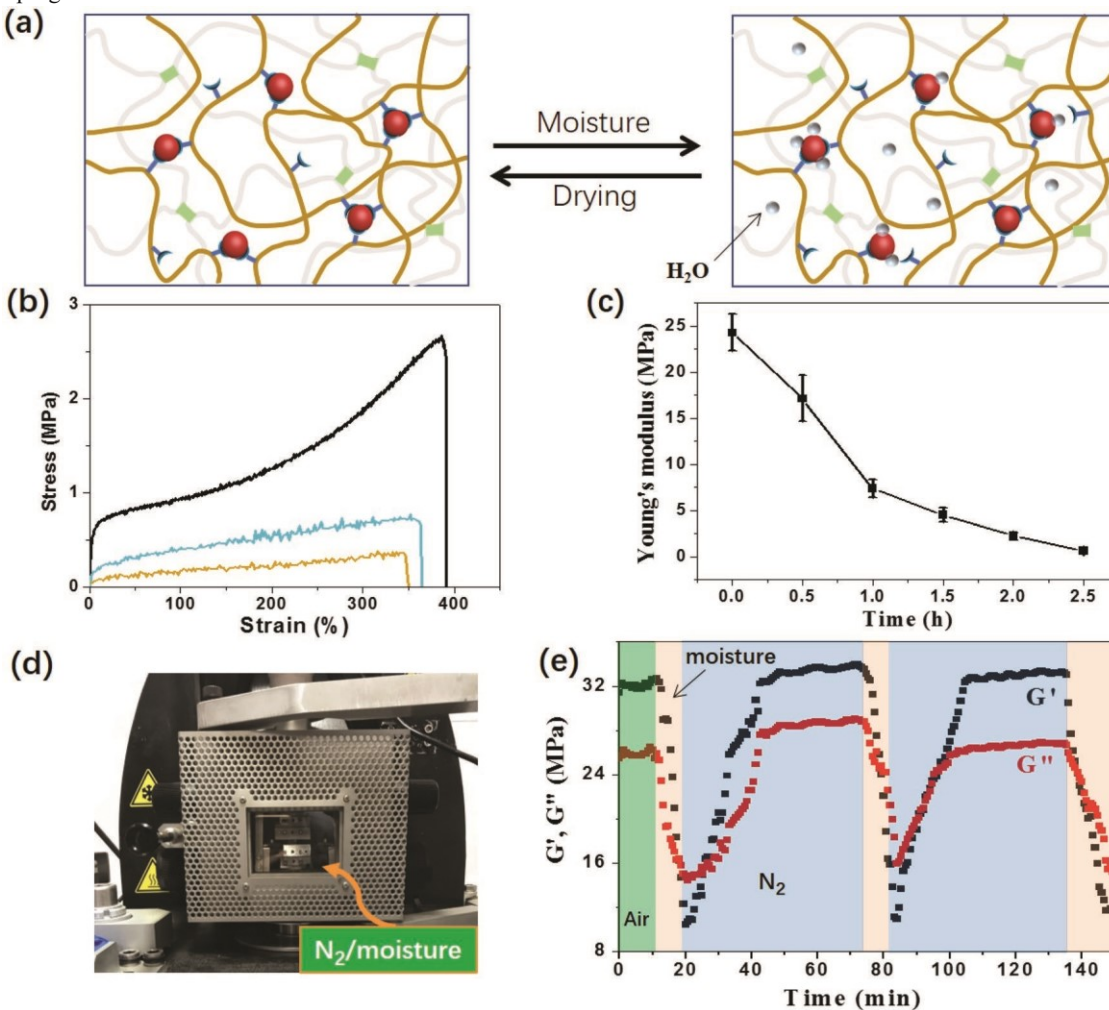


Figure 5. Moisture-controlled mechanical properties of the Eu-containing polymer elastomer. a) Scheme illustrating the reversible disruption/reformation of the Eu-IDA coordination in the two networks under moisture-dry cycles. The covalently cross-linked P(AA-*co*-nBA) is drawn in light gray to make it distinguishable with the physical cross-linking network provided by Eu-IDA coordination in P(MEO₂MA-*co*-IDHPMA) (orange). b) Stress-strain curves of the Eu-containing polymer films subject to 0 h (black), 1.5 (blue) and 2.5 h (orange) of moisture at an RH of 80%. c) E of the polymer films plotted against exposure time. d) An optical image showing apparatus for the dynamic mechanical measurement in a closed chamber alternatively purged with N₂/water-saturated air. A more detailed scheme of this apparatus is given in Figure S11 (Supporting Information). e) Moisture-driven switch between “elastic solid” and “viscous fluid” states. At the initial stage, the polymer film was measured in air (green region). The DMA measurement was carried out under a frequency of 5 Hz and a strain of 1%. All samples have an IDA-to-Eu ratio of 14.7 MPa after 8 min, respectively, where the sample behaves as a viscous fluid. This corresponds to the disappearance of high stiffness and toughness of the film under uniaxial tensile measurement. By subsequently purging with dry N₂, a steep upturn of G' and G'' was seen. The moduli increased steadily until they reach plateau at 23 min of dry N₂ purge, where $G' = 33$ MPa and G''

modulus, this

polymer film only gives a G' and G'' decreasing of $\approx 22\%$ and $\approx 16\%$ during moisture-purging process, respectively. However, the Eu-containing polymer film shows a much larger G' and G'' change ($\approx 68\%$ and $\approx 43\%$, respectively). It suggests that the switching of

mechanical states is mainly resulted from the moisture-induced disruption and reformation of Eu-IDA coordination. Considering that the Eu-containing elastomer film has much pronounced modulus change that switches the mechanical states of polymer from elastic solid to viscous liquid. This does not exist in the polymer film without Eu³⁺ ions where the plasticizing effect of water only shows limit influences. We note that, moisture is one of many other stimuli that can dynamically control the coordination of Eu-IDA.^[12a] Other stimuli like the change of pH/temperature/ionic strength/sonication that potentially disrupt the Eu-IDA coordination, can result in the similar response of mechanical strength and toughness.

3. Conclusion

In summary, we demonstrated a tough polymer elastomer with intriguing moisture-controlled fluorochromic and mechanical response. The dynamic nature of Eu-IDA complexation that allows reversible coordination/dissociation upon stretching the elastomer enabled the stress relaxation and the energy dissipation as tough elastomers. We showed that the incorporation of Eu-IDA complexation in an IPN polymer could dramatically enhance the strength and toughness of the polymer film. Even with a low content of Eu³⁺ ions (the mole ratio of IDA-to-Eu 7/1), the *E* of the tough polymer film reached 24.3 MPa, one order of magnitude higher than that of the film without Eu³⁺ ions. The Eu-containing polymer elastomer was highly transparent and showed “ON/OFF” switchable red emission of Eu³⁺ ions by pH, ions and moisture. The large Eu³⁺ ions also favored the coordination with water in its first coordination sphere, leading to moisture-responsive optical and mechanical properties of the elastomer. By balancing with an appropriate amount of fluorescein in the Eu-containing elastomer, the white-emitting elastomer film showed distinct and reversible color change under moisture-dry cycles. The incorporation of water in the coordination sphere of Eu³⁺ ions consequently gave an interesting impact on the mechanical strength and toughness of the Eu-containing film. The toughness, as well as the mechanical states between viscous fluid and elastic solid, could be reversibly switched by moisture as an external stimulus. We expect that this fluorochromic tough elastomer will pave a new way for preparing elastomers with high mechanical performance and expand their applications in anticounterfeiting coating and multistimuli-responsive materials both optically and mechanically.

4. Experimental Section

Materials: Iminodiacetic acid and Eu(NO₃)₃ · 6H₂O were supplied by Adamas Reagent. Di(ethylene glycol) methyl ether methacrylate (MEO₂MA), glycidyl methacrylate (GMA), 2,2'-azobis(isobutyronitrile) (AIBN), *n*-butyl acrylate (*n*-BA), acrylic acid (AA), ethylene glycol dimethacrylate (EGDMA), 2-hydroxy-2-methyl-1-phenylpropan-1-one (photoinitiator), and fluorescein were purchased from TCI. MEO₂MA, GMA, and *n*-BA were passed through a basic aluminum oxide column prior to use. AIBN was recrystallized twice from ethanol. All solvents were purchased from commercial sources and used as received. Deionized water with a resistivity of >18.0 MΩ cm was used to prepare IDA and Eu(NO₃)₃ aqueous solution.

Polymer Synthesis: The copolymer of MEO₂MA and GMA was prepared by free radical copolymerization. MEO₂MA (30 g, 160 mmol), GMA (4.54 g, 32 mmol), and AIBN (26.2 mg, 160 μmol) were dissolved in 30 mL anisole in

a 100 mL flask. The reaction mixture was degassed under vacuum and filled with nitrogen for 15 min. The flask was then sealed and placed in a pre-heated oil bath at 65 °C for 5 h. After reaction, the mixture was cooled down to room temperature. The polymer was collected after precipitation in hexane three times and dried under vacuum for 24 h. The obtained polymer had a number-average molecular weight (*M*_n) of 127.8 kg mol⁻¹ and a dispersity (\mathcal{D}) of 3.62 (Figure S1, Supporting Information), measured by size exclusion chromatography (SEC) using polystyrene (PS) standards.

The copolymer P(MEO₂MA-*co*-GMA) with 16.7 mol% of GMA units was functionalized by IDA through the ring opening reaction of epoxide moieties.^[17] Before the reaction iminodiacetic acid was neutralized with excess NaOH aqueous solution to avoid carboxylic acid reacting with epoxy. Typically, P(MEO₂MA-*co*-GMA) (5 g, 4.6 mmol for the GMA unit) was first dissolved in 88 mL of mixed solvent of methanol/*N,N*'-dimethylformamide (10/1, v/v). Then, the sodium salt of iminodiacetic acid aqueous solution (20 wt%, 6.1 mL, 9.2 mmol) was added dropwise into the P(MEO₂MA-*co*-GMA) solution and refluxed at 65 °C overnight to yield poly(di(ethylene glycol) methyl ether methacrylate-*co*-3-iminodiacetate-2-hydroxypropylmethacrylate) (P(MEO₂MA-*co*IDHPMA)). After reaction, the polymer solution was first precipitated in ethanol. The polymer was then redissolved in mixed solvent of methanol/ dioxane (10/1, v/v) and precipitated in cold diethyl ether for three times. After precipitation, the polymer was dried under vacuum for 24 h.

Preparation of Eu-Containing Organogels and IPN Elastomeric Films: To prepare a typical P(MEO₂MA-*co*-IDHPMA) organogel with an IDA-to-Eu molar ratio of 7/1, 0.2 g P(MEO₂MA-*co*-IDHPMA) was first dissolved in 1.9 mL mixed solvent of methanol/dioxane (10/1, v/v). Then, 101 μL of 10 wt% Eu(NO₃)₃ aqueous solution was mixed with the polymer solution in a vial and shook by a vortexer for 1 min. The mixture was sealed and incubated under room temperature for 24 h to yield a transparent organogel. Eu-containing organogels with different IDA-to-Eu ratios were prepared by using similar procedures.

A 10 wt% of P(MEO₂MA-*co*-IDHPMA) solution was first prepared by dissolving the polymer in mixed solvent of methanol/dioxane (10/1, v/v). To prepare a typical Eu-containing IPN elastomer (IDA-to-Eu ratio of 7/1, mol/mol), 0.016 g of EGDMA, 0.108 g of *n*-BA, 0.546 g of AA, and 0.011 g of photoinitiator were first mixed with 2 mL of the P(MEO₂MA-*co*-IDHPMA) solution. Subsequently, 101 μL of 10 wt% Eu(NO₃)₃ aqueous solution was added in a vial and vortexed for 1 min to form the first physically cross-linked P(MEO₂MA-*co*-IDHPMA) network. The viscous mixture was then transferred to a syringe and sealed. After incubated for 5 h under room temperature in the dark, the uniform mixture was transferred to a Petri dish and pressed carefully into a thin liquid film by a transparent plastic cover. The plastic cover was left on the top of the liquid film to avoid evaporation of the solvent and exclude the influence of oxygen from the air. After a 20 min of UV irradiation, a film-like organogel was obtained. Here, the UV light triggered copolymerization of *n*-BA and AA in the presence of EGDMA as a chemical cross-linker generated the second covalently cross-linked network. Finally, the IPN structure was obtained. A scheme is included in Figure S2b (Supporting Information) to show the fabrication of the IPN structure. This film-like organogel was then dried under vacuum at 60 °C for 24 h to obtain the Eu-containing IPN elastomeric film with a thickness of 0.4 mm. Using similar procedures, Eu-containing IPN elastomeric films with different IDA-to-Eu ratios were prepared.

To prepare a white-light-emitting IPN elastomeric film, greenemissive fluorescein was first dissolved in mixed solvent of methanol/ dioxane (10/1, v/v) to obtain a 0.1 wt% fluorescein solution. Using the same procedure in 3.2, 163 μL of 0.1 wt% fluorescein solution was added before the addition of 101 μL of 10 wt% Eu(NO₃)₃ aqueous solution. Finally, the white-emitting IPN elastomeric film (IDA-to-Eu ratio of 7/1) had a fluorescein/Eu³⁺ molar ratio of 1/46. For comparison, fluorescein-containing elastomeric film was also prepared with an IDA-to-fluorescein molar ratio of 322/1.

Characterization: UV irradiation experiments for the preparation of IPN elastomeric films were carried out using a 365 nm UV lamp (UV-20A, Shanghai-Yaozhuang) with a light intensity of 1 mW cm^{-2} . Fluorescence emission of all samples was visualized under a UV lamp (ZF-7A, Shanghai-Gucun).

The SEC instrument package was supplied by Shimadzu and comprised the following setup: a Shimadzu LC-20AD pump, two series of connected columns (Shodex, K-803 and K-804) in a Shimadzu CTO-20 oven at 35°C , and a Shimadzu RID-10A refractive index detector. Tetrahydrofuran was used as the mobile phase at a flow rate of 1 mL min^{-1} at 40°C and the molecular weight was calibrated against polystyrene standards. Proton nuclear magnetic resonance ($^1\text{H NMR}$) spectra were recorded on a Bruker Ascend 400 MHz spectrometer using CDCl_3 and D_2O as the solvent for P(MEO₂MA-co-GMA) and P(MEO₂MAco-IDHPMA), respectively.

A Haake Mars III rheometer was used to perform rheological tests. Frequency sweep (strain = 1%) spectra of the P(MEO₂MA-co-IDHPMA) organogels with different IDA-to-Eu ratios were performed on a 20 mm parallel plate and the frequency ranges from 0.01 to 100 rad s^{-1} . Photocross-linking kinetics of the Eu-containing IPN elastomer (IDA-to-Eu ratio of 7/1) was measured by a time sweep under constant oscillating frequency of 1 rad s^{-1} and strain of 1%. To conduct these measurements, all starting materials were mixed and divided into 14 testing samples. Samples subject to different UV irradiation times (0, 1, 2, 3, 4, 5, 6, 8, 10, 12, 14, 16, 18, and 20 min) were immediately transferred to the rheometer for time sweep measurements. Each sample underwent 5 min of time sweep to obtain steady G' and G'' values. All measurements were conducted at 25°C . A solvent trap was used to minimize the evaporation of solvent.

The fluorescence spectra were recorded by an OHSP-350s spectrophotometer (Hopoo, Hangzhou, China). The schematic drawing for this measurement is shown in Figure S3 (Supporting Information). Using the same procedure, the elastomer films were prepared in a transparent plastic Petri dish. The Petri dish with the elastomer film was then placed over the detector of the spectrophotometer. The emission spectra of all luminescent IPN elastomeric films excited by the ZF-7A 365 nm UV lamp were recorded under UV irradiation. A specific spectral band was isolated using a band-pass filter at $365 \pm 10 \text{ nm}$ throughout the fluorescence measurements. Fluorescence lifetime of the Eu-containing elastomer film was measured by an FLS 980 spectrophotometer (Edinburgh Instruments, UK) at room temperature by monitoring the emission decay at 617 nm. The obtained spectrum was fitted with a biexponential function. The quantum yield was measured using Rhodamine B as a standard with a known quantum yield^[23] (68% in ethanol at an excitation wavelength of 365 nm^[24]).

SAXS measurements were performed using a Xeuss SAXS system (Xenocs SA) with Cu K α radiation (wavelength = 0.154 nm). The sample-to-detector distance was 2550 mm. The SAXS pattern was recorded by a Mar 345 image plate as a detector. The SAXS pattern was background corrected and then integrated to obtain the 1D scattering curve.

Uniaxial tensile tests were conducted on an MTS Criterion Model 43 material testing machine with a loading cell of 1000 N. The specimen was a dumbbell shaped thin strip ($30 \times 10 \times 0.4 \text{ mm}^3$) and experiments were performed with a tensile speed of 50 mm min^{-1} . Stress relaxation tests were carried out by holding samples at a strain of 100% for 20 min. Cyclic-loading experiments were held at zero force between cycles by reducing the applied strain as specimens contracted. Using the same tensile speed of 50 mm min^{-1} , uniaxial tensile tests were carried out. All mechanical tests were carried out at 25°C and a relative humidity of 55% in the environmental chamber.

Eu-containing IPN elastomeric films with a diameter of 25 mm and a thickness of 0.4 mm were prepared. A writing brush soaked in 5 wt% $\text{Fe}(\text{NO}_3)_3/1 \text{ M HCl}$ aqueous solution was used to write "Eu" on the films. The writing script by HCl was erased through applying 1 M NaOH aqueous solution on the written film. After drying the NaOH-solution treated film, the fluorescence can be fully recovered.

Rectangular sample films with a dimension of $20 \times 10 \times 0.4 \text{ mm}$ were used for fluorochromic tests. An LHP-160 (Ronghua instrument, Changzhou, China) constant temperature and humidity cultivation cabinet was used to supply different humidity (RH 50%, 65%, and 80%) at 25°C . At selected incubation times, samples were immediately taken out and placed over the detector of spectrophotometer for fluorescence measurements. Samples were dried by purging dry N_2 for fluorescence recovery.

Using the MTS Criterion Model 43 material testing machine and similar procedure mentioned in 4.5, the influence of humidity on the uniaxial tensile performance of the Eu-containing IPN elastomeric film (IDA-to-Eu ratio of 7/1) was investigated. The sample subject to 0, 0.5, 1, 1.5, 2, and 2.5 h at an RH of 80% was incubated in the LHP-160 (Ronghua instrument, Changzhou, China) constant temperature and humidity cultivation cabinet mentioned in 4.7. A Metravib DMA+1000 dynamic mechanical analyzer (DMA) was applied to in situ measure the changes of G' and G'' of the sample in response to alternative switching of N_2 gas/moisture under room temperature under a frequency of 5 Hz and a strain of 1%. The detailed scheme of this measurement is shown in Figure S11 (Supporting Information). The dry N_2 gas and water vapor flew into the testing chamber through a gas input channel. Using two valves, the N_2 gas and moisture-saturated air could be switched easily and quickly. The flow rate (10 L h^{-1}) of the N_2 gas was adjusted by a traces oxygen analyzer (JC 48 V, Setnag, France) and the humidification capacity (0.3 L h^{-1}) of the water vapor was controlled by a humidifier.

Supporting Information

Supporting Information is available from the Wiley Online Library or from the author.

Acknowledgements

X.Z. and L.W. contributed equally to this work. G.W. is grateful for the financial support of the Zhejiang Provincial Natural Science Foundation of China (Grant No. LY19E030002), the Ningbo Municipal Science and Technology Bureau (Grant No. 2017A610051), and the K. C. Wong Magna Fund in Ningbo University. J.H. thanks the financial support from the University of Connecticut and the National Science Foundation (CBET-1705566). This work was partially supported by the Green Emulsions, Micelles and Surfactants (GEMS) Center at the University of Connecticut.

Conflict of Interest

The authors declare no conflict of interest.

Keywords

bioinspired materials, fluorochromic response, moisture sensitive, responsive materials, tough elastomers

Received: May 3, 2019

Revised: June 18, 2019

Published online: July 11, 2019

[1] R. Akashi, H. Tsutsui, A. Komura, *Adv. Mater.* **2002**, *14*, 1808.

- [2] C. Dawson, J. F. Vincent, A.-M. Rocca, *Nature* **1997**, *390*, 668.
- [3] a) J.-Y. Sun, X. Zhao, W. R. K. Illeperuma, O. Chaudhuri, K. H. Oh, D. J. Mooney, J. J. Vlassak, Z. Suo, *Nature* **2012**, *489*, 133; b) L. T. de Haan, J. M. Verjans, D. J. Broer, C. W. Bastiaansen, A. P. Schenning, *J. Am. Chem. Soc.* **2014**, *136*, 10585; c) D. J. Broer, C. M. W. Bastiaansen, M. G. Debije, A. P. H. J. Schenning, *Angew. Chem., Int. Ed.* **2012**, *51*, 7102; d) R. P. Sijbesma, F. H. Beijer, L. Brunsved, B. J. B. Folmer, J. H. K. K. Hirschberg, R. F. M. Lange, J. K. L. Lowe, E. W. Meijer, *Science* **1997**, *278*, 1601.
- [4] a) N. Holten-Andersen, M. J. Harrington, H. Birkedal, B. P. Lee, P. B. Messersmith, K. Y. C. Lee, J. H. Waite, *Proc. Natl. Acad. Sci. USA* **2011**, *108*, 2651; b) J. R. Kumpfer, S. J. Rowan, *J. Am. Chem. Soc.* **2011**, *133*, 12866; c) W. Nan, W. Wang, H. Gao, W. Liu, *Soft Matter* **2013**, *9*, 132; d) M. Mauro, *Eur. J. Inorg. Chem.* **2018**, *2018*, 2090; e) Z. Li, G. Wang, Y. Wang, H. Li, *Angew. Chem.* **2018**, *130*, 2216.
- [5] a) Y. Liu, B. Xu, S. Sun, J. Wei, L. Wu, Y. Yu, *Adv. Mater.* **2017**, *29*, 1604792; b) L. Zhang, X. Qiu, Y. Yuan, T. Zhang, *ACS Appl. Mater. Interfaces* **2017**, *9*, 41599.
- [6] a) R. J. Wojtecki, M. A. Meador, S. J. Rowan, *Nat. Mater.* **2011**, *10*, 14; b) H. Ying, Y. Zhang, J. Cheng, *Nat. Commun.* **2014**, *5*, 3218.

[7] J. L. Silverberg, A. A. Evans, L. McLeod, R. C. Hayward, T. Hull, C. D. Santangelo, I. Cohen, *Science* **2014**, *345*, 647.

[8] M. Vatankhah-Varnosfaderani, A. N. Keith, Y. Cong, H. Liang, M. Rosenthal, M. Sztucki, C. Clair, S. Magonov, D. A. Ivanov, A. V. Dobrynin, S. S. Sheiko, *Science* **2018**, *359*, 1509.

[9] a) J. B. Beck, S. J. Rowan, *J. Am. Chem. Soc.* **2003**, *125*, 13922; b) S. V. Eliseeva, J. C. Bunzli, *Chem. Soc. Rev.* **2010**, *39*, 189; c) K. Binnemans, *Coord. Chem. Rev.* **2015**, *295*, 1; d) J. Hai, T. Li, J. Su, W. Liu, Y. Ju, B. Wang, Y. Hou, *Angew. Chem., Int. Ed.* **2018**, *57*, 6786.

[10] J. Kuta, A. E. Clark, *Inorg. Chem.* **2010**, *49*, 7808.

[11] a) H. S. Jung, P. Verwilst, W. Y. Kim, J. S. Kim, *Chem. Soc. Rev.* **2016**, *45*, 1242; b) F. Gao, F. Luo, X. Chen, W. Yao, J. Yin, Z. Yao, L. Wang, *Microchim. Acta* **2009**, *166*, 163; c) L. Song, Y. W. Wu, W. X. Chai, Y. S. Tao, C. Jiang, Q. H. Wang, *Eur. J. Inorg. Chem.* **2015**, *2015*, 2264; d) L. N. Neumann, C. Calvino, Y. C. Simon, S. Schrettli, C. Weder, *Dalton Trans.* **2018**, *47*, 14184.

[12] a) G. Weng, S. Thanneeru, J. He, *Adv. Mater.* **2018**, *30*, 1706526; b) P. Chen, Q. Li, S. Grindy, N. Holten-Andersen, *J. Am. Chem. Soc.* **2015**, *137*, 11590; c) D. W. Balkenende, S. Coulibaly, S. Balog, Y. C. Simon, G. L. Fiore, C. Weder, *J. Am. Chem. Soc.* **2014**, *136*, 10493; d) M. Martinez-Calvo, O. Kotova, M. E. Mobius, A. P. Bell, T. McCabe, J. J. Boland, T. Gunnlaugsson, *J. Am. Chem. Soc.* **2015**, *137*, 1983; e) Q. Zhu, K. Van Vliet, N. Holten-Andersen, A. Miserez, *Adv. Funct. Mater.* **2019**, *29*, 1808191; f) Y. Zhou, H.-Y. Zhang, Z.-Y. Zhang, Y. Liu, *J. Am. Chem. Soc.* **2017**, *139*, 7168; g) W. Zhou, Y. Chen, Q. Yu, P. Li, X. Chen, Y. Liu, *Chem. Sci.* **2019**, *10*, 3346.

[13] a) A. N. Gent, L. Q. Zhang, *J. Polym. Sci., Part B: Polym. Phys.* **2001**, *39*, 811; b) G. Heinrich, M. Kaliske, *Comput. Theor. Polym. Sci.* **1997**, *7*, 227; c) Z. Tang, J. Huang, B. Guo, L. Zhang, F. Liu, *Macromolecules* **2016**, *49*, 1781; d) G. Weng, H. Yao, A. Chang, K. Fu, Y. Liu, Z. Chen, *RSC Adv.* **2014**, *4*, 43942.

[14] a) T. Q. Trung, N.-E. Lee, *Adv. Mater.* **2016**, *28*, 4338; b) H.-H. Chou, A. Nguyen, A. Chortos, J. W. F. To, C. Lu, J. Mei, T. Kurosawa, W.-G. Bae, J. B. H. Tok, Z. Bao, *Nat. Commun.* **2015**, *6*, 8011.

[15] a) M. K. Choi, J. Yang, K. Kang, D. C. Kim, C. Choi, C. Park, S. J. Kim, S. I. Chae, T.-H. Kim, J. H. Kim, T. Hyeon, D.-H. Kim, *Nat. Commun.* **2015**, *6*, 7149; b) M. K. Choi, I. Park, D. C. Kim, E. Joh, O. K. Park, J. Kim, M. Kim, C. Choi, J. Yang, K. W. Cho, *Adv. Funct. Mater.* **2015**, *25*, 7109.

[16] a) H. Hu, J. Tang, H. Zhong, Z. Xi, C. Chen, Q. Chen, *Sci. Rep.* **2013**, *3*, 1484; b) S. Han, H. J. Bae, J. Kim, S. Shin, S. E. Choi, S. H. Lee, S. Kwon, W. Park, *Adv. Mater.* **2012**, *24*, 5924.

[17] S. Thanneeru, S. S. Duay, L. Jin, Y. Fu, A. M. Angeles-Boza, J. He, *ACS Macro Lett.* **2017**, *6*, 652.

[18] A. S. Chauvin, F. Gumy, D. Imbert, J. C. G. Bünzli, *Spectrosc. Lett.* **2004**, *37*, 517.

[19] a) C.-H. Li, C. Wang, C. Keplinger, J.-L. Zuo, L. Jin, Y. Sun, P. Zheng, Y. Cao, F. Lissel, C. Linder, X.-Z. You, Z. Bao, *Nat. Chem.* **2016**, *8*, 618; b) E. Filippidi, T. R. Cristiani, C. D. Eisenbach, J. H. Waite, J. N. Israelachvili, B. K. Ahn, M. T. Valentine, *Science* **2017**, *358*, 502; c) E. Ducrot, Y. Chen, M. Bulters, R. P. Sijbesma, C. Creton, *Science* **2014**, *344*, 186.

[20] a) J. Wu, L. H. Cai, D. A. Weitz, *Adv. Mater.* **2017**, *29*, 1702616; b) R. E. Webber, C. Creton, H. R. Brown, J. P. Gong, *Macromolecules* **2007**, *40*, 2919; c) H. R. Brown, *Macromolecules* **2007**, *40*, 3815.

[21] a) G. R. Choppin, D. R. Peterman, *Coord. Chem. Rev.* **1998**, *174*, 283; b) T. Ozaki, M. Arisaka, T. Kimura, A. Francis, Z. Yoshida, *Anal. Bioanal. Chem.* **2002**, *374*, 1101.

[22] a) H. Levine, L. Slade, *Water Sci. Rev.* **1988**, *3*, 79; b) P. Blasi, S. S. D'Souza, F. Selmin, P. P. DeLuca, *J. Controlled Release* **2005**, *108*, 1.

[23] G. A. Crosby, J. N. Demas, *J. Phys. Chem.* **1971**, *75*, 991.

[24] V. Bhalla, R. Tejpal, M. Kumar, *Sens. Actuators, B* **2010**, *151*, 180.

1903543